

MYELOID NEOPLASIA

Distinct effects of concomitant *Jak2V617F* expression and *Tet2* loss in mice promote disease progression in myeloproliferative neoplasms

Edwin Chen,¹ Rebekka K. Schneider,¹ Lawrence J. Breyfogle,¹ Emily A. Rosen,¹ Luke Poveromo,¹ Shannon Elf,¹ Amy Ko,¹ Kristina Brumme,¹ Ross Levine,² Benjamin L. Ebert,^{1,3} and Ann Mullally^{1,3}

¹Division of Hematology, Department of Medicine, Brigham and Women's Hospital, Harvard Medical School, Boston, MA; ²Human Oncology and Pathogenesis Program, Memorial Sloan-Kettering Cancer Center, New York, NY; and ³Broad Institute, Cambridge, MA

Key Points

- *Tet2* loss of function confers a strong functional competitive advantage to *Jak2V617F*-mutant hematopoietic stem cells.
- *Jak2V617F* expression and *Tet2* loss generate distinct and nonoverlapping transcriptional programs in hematopoietic stem cells.

Signaling mutations (eg, *JAK2V617F*) and mutations in genes involved in epigenetic regulation (eg, *TET2*) are the most common cooccurring classes of mutations in myeloproliferative neoplasms (MPNs). Clinical correlative studies have demonstrated that *TET2* mutations are enriched in more advanced phases of MPNs such as myelofibrosis and leukemic transformation, suggesting that they may cooperate with *JAK2V617F* to promote disease progression. To dissect the effects of concomitant *Jak2V617F* expression and *Tet2* loss within distinct hematopoietic compartments in vivo, we generated *Jak2V617F/Tet2* compound mutant genetic mice. We found that the combination of *Jak2V617F* expression and *Tet2* loss resulted in a more florid MPN phenotype than that seen with either allele alone. Concordant with this, we found that *Tet2* deletion conferred a strong functional competitive advantage to *Jak2V617F*-mutant hematopoietic stem cells (HSCs). Transcriptional profiling revealed that both *Jak2V617F* expression and *Tet2* loss were associated with distinct and nonoverlapping gene expression signatures within the HSC compartment. In aggregate, our findings indicate that *Tet2* loss drives clonal dominance in HSCs,

and *Jak2V617F* expression causes expansion of downstream precursor cell populations, resulting in disease progression through combinatorial effects. This work provides insight into the functional consequences of *JAK2V617F-TET2* comutation in MPNs, particularly as it pertains to HSCs. (*Blood*. 2015;125(2):327-335)

Introduction

Whole-genome and whole-exome sequencing studies have provided important insight into the somatic genetic lesions that drive myeloid neoplasms.¹⁻³ Although much can be inferred from the patterns of genetic alterations identified in such studies, we still have an incomplete understanding of the functional significance of these relationships, particularly in how different driver mutations collaborate in the transformation of the hematopoietic stem cell (HSC).

In myeloproliferative neoplasms (MPNs), the majority of driver mutations can be broadly classified within two categories.⁴ First, virtually all MPN patients are now known to harbor mutations that confer hyperactive JAK-STAT signaling. By far, the *JAK2V617F* mutation is the most frequent of these mutations,⁵⁻⁸ with a minority of patients also harboring mutations in exon 12 of *JAK2*,⁹ *MPL*,¹⁰ *LNK*,¹¹ or *c-CBL*.¹² Recently, mutations in the gene encoding the endoplasmic reticulum chaperone, calreticulin (*CALR*) have been identified in the majority of *JAK2*-unmutated MPN patients,^{3,13} with early evidence suggesting that mutant *CALR* also causes constitutive JAK-STAT signaling and cytokine-independent growth.¹³

The second major class of somatic alterations in the MPN cancer genome is in genes encoding epigenetic regulators.¹⁴ In particular,

deletions or loss-of-function mutations of the *TET2* methylcytosine dioxygenase occur in approximately 7.5% to 17% of MPNs and are enriched in myelofibrosis compared to essential thrombocythemia^{15,16} and more aggressive forms of mastocytosis.¹⁷ Other than *JAK2V617F* and mutations in *CALR*, *TET2* is the most common somatically altered gene in MPNs and the most commonly comutated gene with *JAK2V617F*.¹⁸ Although *JAK2V617F* and *CALR* mutations are mutually exclusive, *TET2* mutations cooccur with both,¹⁹ suggesting that *TET2* impacts distinct downstream oncogenic pathways from those affected by *JAK2V617F* or mutant *CALR*.

MPN animal models accurately recapitulate human disease in mice and have been an important tool for the study of MPN biology and therapy.^{20,21} Genetically engineered *Jak2V617F* and *Tet2* animal models generated by ourselves and others^{20,21} have permitted a detailed examination of the functional effects of these genetic alterations in different hematopoietic compartments. In this study, we sought to model the co-occurrence of *JAK2V617F* and *TET2* mutations in MPN patients by investigating the consequences of concomitant *Jak2V617F* expression and *Tet2* loss in vivo. We provide new insight into the impact of *Tet2* loss

Submitted April 2, 2014; accepted September 8, 2014. Prepublished online as *Blood* First Edition paper, October 3, 2014; DOI 10.1182/blood-2014-04-567024.

The online version of this article contains a data supplement.

There is an Inside *Blood* Commentary on this article in this issue.

The publication costs of this article were defrayed in part by page charge payment. Therefore, and solely to indicate this fact, this article is hereby marked "advertisement" in accordance with 18 USC section 1734.

© 2015 by The American Society of Hematology

on (1) disease progression in *Jak2V617F*-mediated MPNs; (2) *Jak2V617F*-mutant hematopoietic stem and progenitor cell (HSPC) function; and (3) the transcriptional program of *Jak2V617F*-mutant MPN stem cells.

Material and methods

Experimental mice

We have previously described *Jak2V617F* ($Jak2^{VF}$) conditional knockin and *Tet2* conditional knockout mice.^{22,23} In this study, we used VavCre transgenic mice to target Cre recombinase expression to the hematopoietic lineage²⁴ and to delete *Tet2* in the hematopoietic compartment of *Jak2V617F* mice (supplemental Figure 1). We generated $Jak2^{VF}$ mice that were wild-type (WT) or nullizygous for *Tet2* ($Jak2^{VF}$ or $Jak2^{VF}/Tet2^{null}$, respectively). We also generated mice that were WT for *Jak2* and nullizygous for *Tet2* ($Tet2^{null}$). For controls, we used VavCre-positive mice that were WT for both *Jak2* and *Tet2*. We maintained all mice in pathogen-free facilities at Children's Hospital Boston. The institutional ethics committee of Children's Hospital Boston approved all mouse experiments on protocol 13-04-2393R.

Blood analysis

Blood was collected into EDTA-coated containers and analyzed on a Hemavet 950 analyzer (Drew Scientific).

Flow cytometry

Bone marrow, spleen, or peripheral blood was collected and prepared for staining by red blood cell lysis (BD Pharm Lyse; BD Biosciences) and homogenization through a 70- μ m filter. Erythroid precursor cell stainings were not pretreated with red cell lysis. All samples were analyzed by flow cytometry using the fluorescence-activated cell sorter BD FACSCanto or BD LSR II (BD Biosciences). All staining steps were performed in ice-cold phosphate-buffered saline containing 2% fetal bovine serum. Postacquisition analysis of data was performed with FlowJo software V9.2.3 (Tree Star, Ashland, OR). For peripheral blood chimerism studies, the following antibodies were used (clone in parentheses): CD45.1 (A20) and CD45.2 (104). For erythroid precursor cells, the following antibodies were used: CD71 (R17217) and Ter119 (Ter-119). For stem cell and progenitor analysis, the following antibodies were used: a lineage cocktail containing CD3 ϵ (145-2C11), CD5 (53-7.3), Ter-119 (TER-119), Gr-1 (RB6-8C5), Mac-1 (M1/70), and B220 (30-F11); c-Kit (2B8), Sca-1 (D7), CD150 (TC15-12F12.2), CD48 (HM48-1), CD135 (A2F10), CD34 (Ram34), and CD16/32 (93), in addition to CD45.1 (A20) and CD45.2 (104). For dead cell discrimination, SYTOX Blue (Invitrogen) was used. For cell cycle analysis, cells were first stained for lineage, stem, and progenitor markers, then fixed and permeabilized and stained with Ki67, followed by staining with Hoechst 33342. For cell sorting experiments, lineage-positive cells were first depleted with Dynabeads (Invitrogen); c-Kit positive cells were first enriched using CD117 mouse microbeads using magnetic-activated cell sorting (Miltenyi Biotec). The remaining cells were then stained with biotinylated lineage cocktail antibodies (clones listed above), followed by Streptavidin-ApcCy7, cKit (2B8), Sca-1 (D7), CD150 (TC15-12F12.2), and CD48 (HM48-1) where appropriate, and sorted on a BD FACSAria cell sorter (BD Biosciences).

Histopathology

Tissues were fixed in 10% neutral buffered formalin, embedded in paraffin, and stained with hematoxylin-eosin (H&E), or with reticulin when assessing for fibrosis. For megakaryocyte analysis, megakaryocytes were counted in 10 high-power fields ($\times 1000$ with oil) per tibia from 4 biological replicates. Images of histologic slides were obtained on a Nikon Eclipse E400 microscope (Nikon, Tokyo, Japan) equipped with a SPOT RT color digital camera, model 2.1.1 (Diagnostic Instruments, Sterling Heights, MI).

Colony-forming unit assays

Myeloid colony-plating assays were performed in methylcellulose-based medium supplemented with complete cytokine mix (MethoCult GF M3434; Stem Cell Technologies). We plated unfractionated bone marrow cells in methylcellulose-based medium, seeded 1×10^4 cells per plate in triplicate, and scored for colony formation 7 to 10 days later. For serial replating assays, we resuspended, pooled, and washed the remaining cells of the same genotype in phosphate-buffered saline (Gibco). We then counted the cells and replated 1×10^4 cells in triplicate under the same culture conditions as previously and scored colonies 7 to 10 days later. We performed serial replating a total of 4 times.

Bone marrow transplantation

Bone marrow cells were resuspended in Hanks balanced salt solution (Gibco) and injected into lethally irradiated (1×10 Gy [1000 rads]) WT recipient mice by either lateral tail vein or retroorbital injection.

Competitive transplantation experiments were performed using lineage^{low}Kit^{high}Sca1⁺ (LSK) cells purified from $Jak2^{VF}$, $Tet2^{null}$, or $Jak2^{VF}/Tet2^{null}$ mice ($n = 2$ pooled for each genotype) and WT LSK cells isolated from 45.1 mice. LSK cells were mixed and then injected into lethally irradiated 45.1 SJL recipients ($n = 5$ in each recipient group). On a single-mouse basis, 2.5×10^4 $Jak2^{VF}$ LSK cells were competed against 1.43×10^4 WT 45.1 LSK cells (ratio 1.7:1; 64% $Jak2^{VF}$, 36% WT); 1.65×10^4 LSK $Tet2^{null}$ LSK cells were competed against 2.3×10^4 WT 45.1 LSK cells (ratio 0.7:1; 42% $Tet2^{null}$, 58% WT); 2.0×10^4 $Jak2^{VF}/Tet2^{null}$ LSK cells were competed against 2.0×10^4 WT 45.1 LSK cells (ratio 1:1; 50% $Jak2^{VF}/Tet2^{null}$, 50% WT). Bone marrow derived from *Jak2V617F* and *Tet2* mice expressed the CD45.2 antigen, and WT competitor bone marrow cells expressed 45.1. Of note, because recipient mice also expressed 45.1, residual recipient hematopoietic cells also contributed to hematopoiesis posttransplantation (at an irradiation dose of 10 Gy, we expect approximately 10%-20% residual recipient hematopoiesis).

Purified bone marrow subpopulation transplants were performed using 2.2×10^3 short-term (ST)-HSCs (CD150⁻ CD48⁻ LSK) or 5.0×10^3 multipotent progenitor (MPP) (CD48⁺ LSK) donor cells from $Jak2^{VF}$ or $Jak2^{VF}/Tet2^{null}$ mice ($n = 2$ pooled for each genotype) plus 4×10^5 supportive WT bone marrow cells injected into lethally irradiated 45.1 SJL recipients ($n = 5$ in each recipient group). Bone marrow derived from *Jak2V617F* and *Tet2* mice expressed the CD45.2 antigen; recipient mice and supportive WT bone marrow cells expressed 45.1.

For bone marrow transplantation experiments, percentage chimerism was defined as the proportion of *Jak2V617F* or *Tet2* or *Jak2V617F/Tet2* cells as a percentage of total cells. That is, $(\%CD45.2)/(\%CD45.2 + \%45.1\text{ WT}) \times 100\%$.

Gene expression profiling

LSK cells (3×10^4 to 5×10^4 per mouse) were isolated from WT ($n = 4$), $Tet2^{null}$ ($n = 3$), $Jak2^{VF}$ ($n = 3$), or $Jak2^{VF}/Tet2^{null}$ ($n = 4$) mice. RNA was extracted using a PicoPure RNA isolation kit (Invitrogen) according to the manufacturer's instructions. The samples were amplified with the Illumina TotalPrep RNA Amplification Kit (Invitrogen) and hybridized on Illumina MouseRef-8 v2.0 gene expression arrays. The data were analyzed with GenePattern online analysis software, including quantile normalization.²⁵ Gene set enrichment analysis (GSEA) was performed across the complete list of genes ranked by signal-to-noise ratio according to their differential expression.²⁶ STAT5A and HSC self-renewal signatures were extracted from previously published gene expression data.^{27,28} The microarray data set reported in this article has been deposited in the ArrayExpress repository at European Molecular Biology Laboratory-European Bioinformatics Institute (<http://www.ebi.ac.uk/arrayexpress/>) and is accessible through the ArrayExpress accession number E-MTAB-2986.

Statistical analysis

GraphPad Prism (GraphPad Software, La Jolla, CA) was used to analyze results and create graphs. All comparisons represent 2-tailed unpaired

Student *t* test analysis (using the Welch correction where appropriate) unless otherwise specified.

Results

Tet2 loss accelerates the MPN phenotype of *Jak2V617F* mice

We have previously described a conditional knockin, which expresses *Jak2V617F* under the control of the endogenous *Jak2* promoter (*Jak2^{VF}* mice).²² The phenotype of the model closely recapitulates many of the clinical features of human MPNs, including prominent splenomegaly as a result of extramedullary hematopoiesis. To evaluate the effect of concomitant *Jak2V617F* expression and *Tet2* loss on MPN phenotype, we generated *Jak2^{VF}/Tet2^{null}* mice and analyzed the splenic phenotype. As previously reported, *Jak2^{VF}* mice exhibited marked splenomegaly (Figure 1A). Strikingly, the spleens of *Jak2^{VF}/Tet2^{null}* mice were significantly larger than those of *Jak2^{VF}* mice (Figure 1A-B). We next performed histopathologic examination of the spleen and found expansion of the white pulp and enlarged partially confluent lymphoid follicles in *Tet2^{null}* mice compared with WT mice (Figure 1C). In contrast, the spleens of *Jak2^{VF}* and *Jak2^{VF}/Tet2^{null}* mice showed marked effacement of the white pulp and trilineage hyperplasia consistent with MPNs (Figure 1C). Similar to *Jak2^{VF}* mice,²² the phenotype of *Jak2^{VF}/Tet2^{null}* mice was apparent at the time of genotyping (1 month), and mice were followed until 6 months of age.

We next assessed the cellular composition of the spleen using flow cytometry and found marked expansion of CD71⁺ Ter119⁺ erythroid precursor cells in *Jak2^{VF}* and *Jak2^{VF}/Tet2^{null}* mice (Figure 1D) and additional expansion of Mac1⁺ Gr1⁺ myeloid precursor cells in the spleens of *Jak2^{VF}/Tet2^{null}* mice compared with *Jak2^{VF}* animals (Figure 1E). Given the marked trilineage hyperplasia that we observed in the spleens of *Jak2^{VF}* and *Jak2^{VF}/Tet2^{null}* mice, we performed a quantitative assessment of the splenic HSC compartment. Compared with WT or *Tet2^{null}* mice, we found expansion of long-term (LT)-HSCs, (ST)-HSCs, and MPP cells in the spleens of *Jak2*-mutant mice irrespective of *Tet2* genotype (Figure 1F). The spleens of *Jak2^{VF}/Tet2^{null}* mice were significantly larger than those of *Jak2^{VF}* animals (Figure 1A), indicating that the splenic LSK compartment of *Jak2^{VF}/Tet2^{null}* mice was expanded absolutely compared with that of *Jak2^{VF}* animals. In aggregate, these data indicate that *Tet2* loss augments the extramedullary hematopoiesis phenotype of *Jak2V617F* mice through additional LSK and myeloid precursor cell expansion, resulting in enhanced splenomegaly.

Tet2 loss influences hematopoietic differentiation within the myeloid progenitor compartment of *Jak2V617F* mice but is insufficient to induce leukemic transformation

To evaluate the effect of *Tet2* loss on the hematopoietic differentiation of *Jak2V617F* mice, we began by analyzing peripheral blood counts. As previously reported, *Jak2V617F* mice demonstrate leukocytosis (Figure 2A), erythrocytosis (Figure 2B and supplemental Figure 2B), and thrombocytosis (Figure 2C and supplemental Figure 2C-D) compared with WT animals. Homozygous loss of *Tet2* led to a trend toward a further elevation in white cell count in mutant *Jak2* mice (Figure 2A), whereas hematocrit and platelet numbers were similarly elevated in both *Jak2^{VF}* and *Jak2^{VF}/Tet2^{null}* animals (Figure 2B-C). More marked leukocytosis developed in *Jak2^{VF}/Tet2^{null}* mice that were older than 6 months (supplemental Figure 2A). Finally, we reviewed

peripheral blood smears and found that platelets from *Jak2^{VF}/Tet2^{null}* mice were large and showed signs of dysplasia, including increased basophilia of the cytoplasm, a tendency to aggregate, abnormal shape, and pseudopod formation (supplemental Figure 2D).

Next, we focused on the bone marrow. We have previously reported that *Jak2V617F* induces erythroid skewing in the myeloid progenitor compartment.²² Consistent with these findings, we found a relative decrease in common myeloid progenitor cells and a relative increase in megakaryocyte-erythroid progenitor cells in the myeloid progenitor bone marrow compartment of *Jak2^{VF}* mice compared with WT mice, which was not seen in *Jak2^{VF}/Tet2^{null}* mice (Figure 2D-F). These findings indicate that *Tet2* loss reduces *Jak2V617F*-induced erythroid skewing in the myeloid progenitor compartment. We also performed a quantitative analysis of HSCs in the bone marrow and found a significant expansion of LT-HSCs in *Tet2^{null}*, *Jak2^{VF}*, and *Jak2^{VF}/Tet2^{null}* mice compared with WT animals, and a significant expansion of MPP cells in *Jak2^{VF}/Tet2^{null}* mice compared with WT animals (supplemental Figure 3A).

TET2 loss-of-function mutations have been associated with leukemic transformation in MPNs.^{18,29-31} Therefore, we compared the propensity for leukemic transformation in *Jak2^{VF}/Tet2^{null}* mice relative to control animals. In the bone marrow of both *Jak2^{VF}* and *Jak2^{VF}/Tet2^{null}* mice, we found trilineage hyperplasia consistent with MPNs, with more prominent myeloid expansion and less prominent erythroid hyperplasia observed in *Jak2^{VF}/Tet2^{null}* marrow relative to *Jak2^{VF}* marrow (Figure 2G-H). We did not see, however, histopathologic evidence of acute myeloid leukemia (AML) in the bone marrow of *Jak2^{VF}/Tet2^{null}* mice up to 6 months old (*n* = 12). Because *Jak2^{VF}* mice die prematurely at approximately 6 months²² and *Jak2^{VF}/Tet2^{null}* mice have a comparable survival, it was not possible to follow *Jak2^{VF}/Tet2^{null}* animals for an extended period beyond 6 months. To further evaluate for leukemic transformation, we measured the percentage of circulating c-Kit⁺ cells using flow cytometry and found no difference between *Jak2^{VF}* and *Jak2^{VF}/Tet2^{null}* animals (supplemental Figure 3B).

Finally, given that *TET2* mutations are enriched in myelofibrosis compared to essential thrombocythemia¹⁶ and that megakaryocytes are a key cellular driver of fibrotic transformation in MPNs,³² we focused on megakaryocytes within the bone marrow of *Jak2^{VF}/Tet2^{null}* mice. We found that the number of megakaryocytes was increased in *Jak2^{VF}/Tet2^{null}* compared with *Jak2^{VF}* mice and that there was greater heterogeneity in megakaryocyte size in *Jak2^{VF}/Tet2^{null}* compared with *Jak2^{VF}* animals (supplemental Figure 4A-B). We next performed a detailed histopathologic analysis and noted emperipolesis and abnormal clustering of megakaryocytes consistent with MPNs in the bone marrow of both *Jak2^{VF}* and *Jak2^{VF}/Tet2^{null}* mice (Figure 2I). With more detailed morphologic analysis, we further noted that *Jak2^{VF}/Tet2^{null}* megakaryocytes appeared apoptotic and showed additional atypical features including pyknotic nuclei and atypical mitotic figures. In aggregate, these findings suggest higher megakaryocyte turnover in *Jak2^{VF}/Tet2^{null}* compared with *Jak2^{VF}* animals (Figure 2I and supplemental Figure 4C). Finally, we performed reticulin staining but did not see evidence of reticulin fibrosis in the bone marrow of *Jak2^{VF}/Tet2^{null}* mice up to 6 months old (*n* = 12) (supplemental Figure 4D).

Tet2 loss confers enhanced self-renewal to *Jak2V617F* bone marrow cells in vitro

Next, we turned to the functional effects of concomitant *Jak2V617F* expression and *Tet2* loss on HSPCs by performing serial replating colony-forming unit assays. We compared colony-forming unit assay

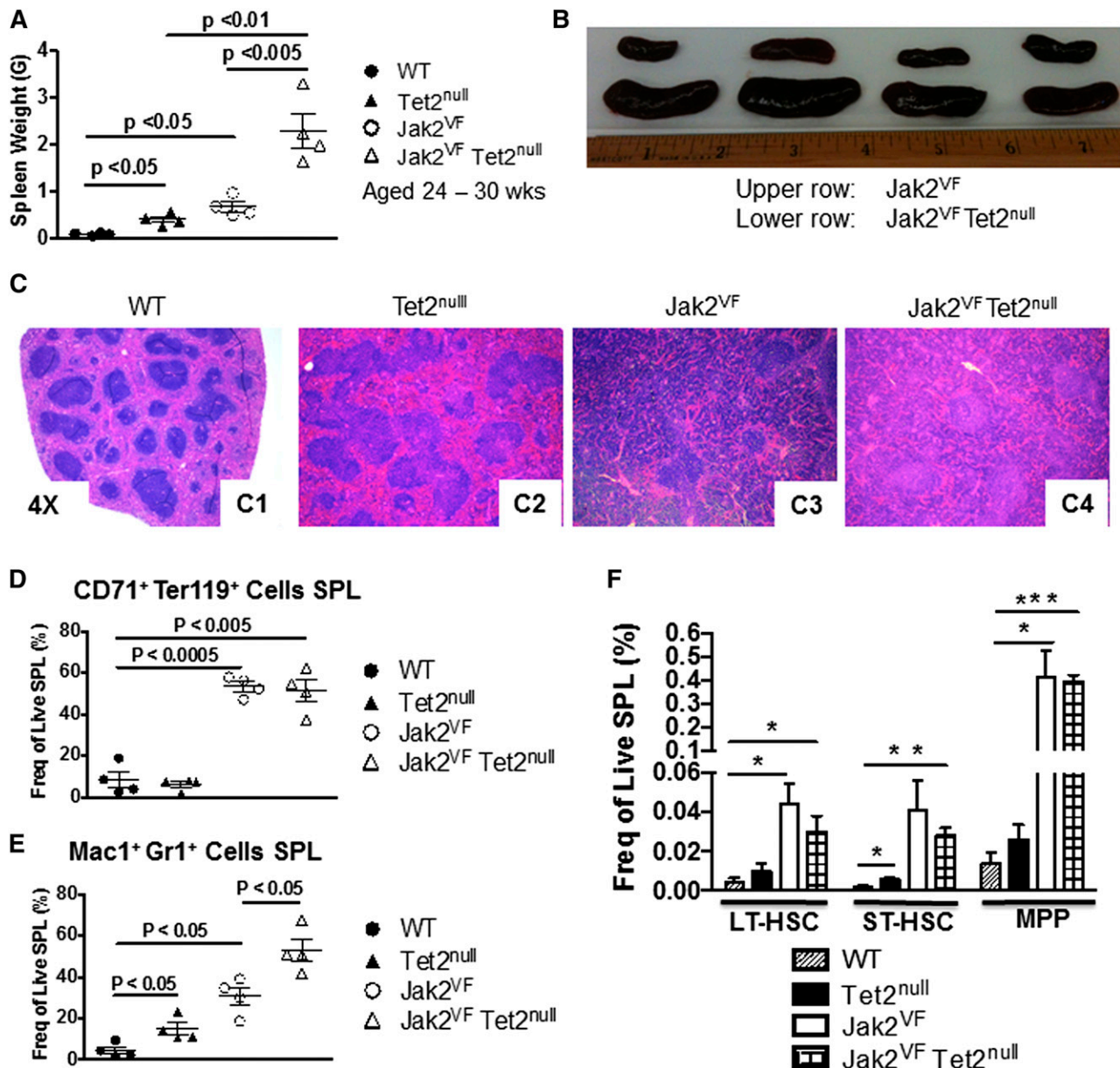


Figure 1. *Tet2* loss accelerates the MPN phenotype of *Jak2*^{V617F} mice. (A) Spleen weights of age-matched WT, *Tet2*^{null}, *Jak2*^{VF}, and *Jak2*^{VF}/*Tet2*^{null} mice 24 to 30 weeks old (mean ± standard error of the mean [SEM]; n = 4 in each group). (B) Photograph of spleens from *Jak2*^{VF} and *Jak2*^{VF}/*Tet2*^{null} mice. (C) Histopathologic sections of spleen from representative WT, *Tet2*^{null}, *Jak2*^{VF}, and *Jak2*^{VF}/*Tet2*^{null} mice (original magnification ×4; H&E stain). (D) Frequency of CD71⁺ Ter119⁺ erythroid precursor cells in spleen from age-matched WT, *Tet2*^{null}, *Jak2*^{VF}, and *Jak2*^{VF}/*Tet2*^{null} mice (mean ± SEM; n = 4 in each group). (E) Frequency of Mac1⁺ Gr1⁺ myeloid precursor cells in spleen from age-matched WT, *Tet2*^{null}, *Jak2*^{VF}, and *Jak2*^{VF}/*Tet2*^{null} mice (mean ± SEM; n = 4 in each group). (F) Frequency of CD150⁺ CD48⁻ LSK cells (LT-HSC), CD150⁻ CD48⁻ LSK cells (ST-HSC), and CD48⁺ LSK cells (MPP) in spleen from age-matched WT, *Tet2*^{null}, *Jak2*^{VF}, and *Jak2*^{VF}/*Tet2*^{null} mice (mean ± SEM; n = 4 in each group). *P < .05; **P < .005; ***P < .001.

formation using unfractionated bone marrow cells derived from *Jak2*^{VF}, *Tet2*^{null}, or *Jak2*^{VF}/*Tet2*^{null} mice. We found that from the third replating onward, *Tet2*^{null} and *Jak2*^{VF}/*Tet2*^{null} cells had markedly enhanced replating activity compared to *Jak2*^{VF} or WT cells (Figure 3A). These findings indicate that homozygous *Tet2* loss confers increased self-renewal potential in vitro to *Jak2*^{V617F}-expressing hematopoietic cells.

***Tet2* loss confers a competitive repopulating advantage to *Jak2*^{V617F} HSCs**

To further evaluate the functional impact of *Tet2* loss on *Jak2*^{V617F} HSCs in vivo, we performed competitive bone marrow transplantation experiments. We transplanted LSK cells derived from *Jak2*^{VF},

Tet2^{null}, or *Jak2*^{VF}/*Tet2*^{null} mice into lethally irradiated congenic recipients, together with an approximately equal number of 45.1 WT competitor LSK cells (see “Materials and methods” for precise ratios). The blood counts were broadly similar in all recipient groups (supplemental Figure 5A-C). We assessed peripheral blood chimerism in total white blood cells, myeloid cells (Gr1⁺), B-lymphoid cells (B220⁺), or T-lymphoid cells (CD3⁺) and found a competitive advantage over WT cells for the *Jak2*^{VF}/*Tet2*^{null} and *Tet2*^{null} cells in each of these compartments (Figure 3B-D and supplemental Figure 5D). This competitive advantage was present at 4 weeks posttransplantation and was sustained at 17 weeks. We assessed chimerism in the bone marrow and spleen at 18 weeks post bone marrow transplantation and found a strong competitive

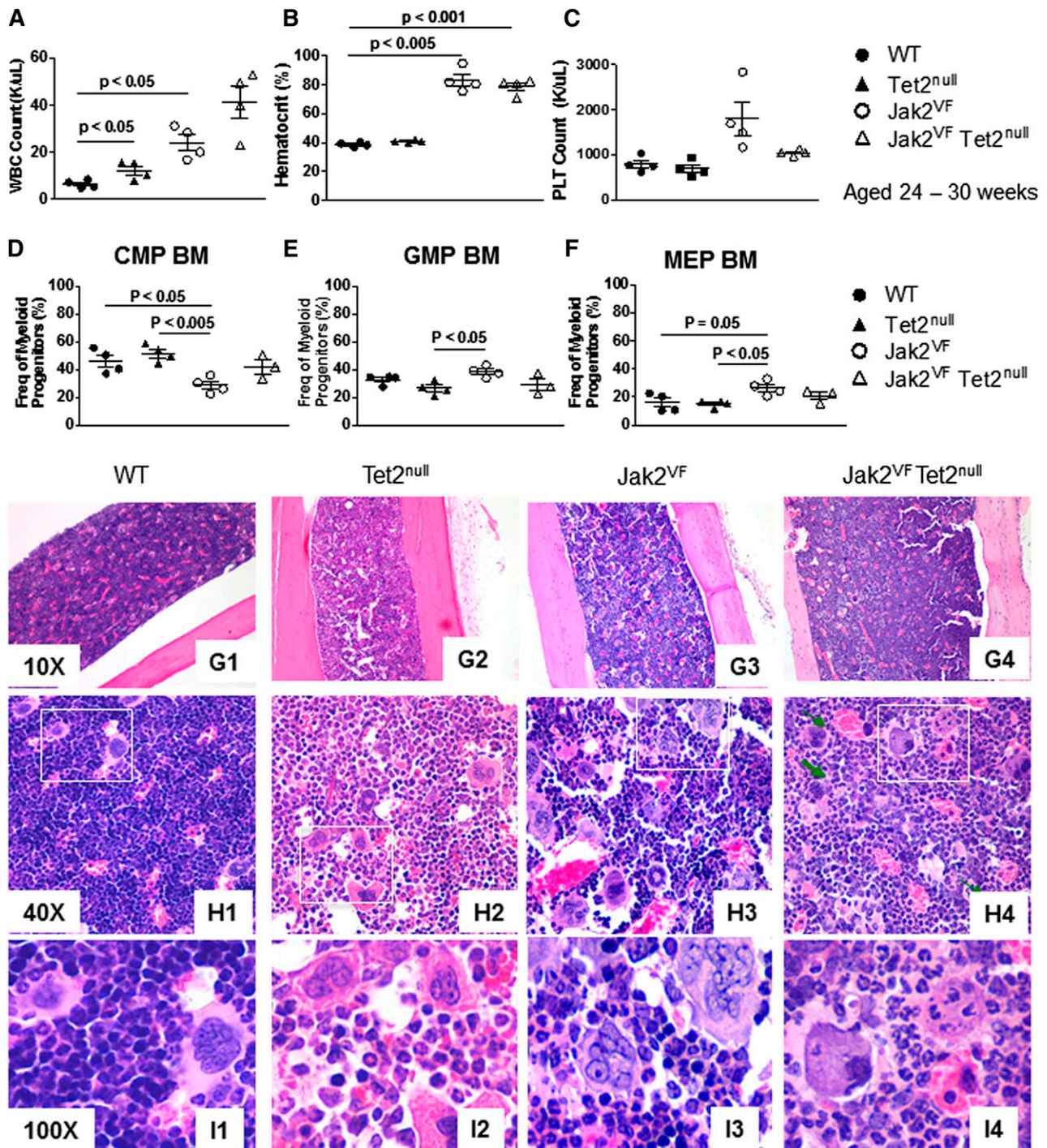


Figure 2. *Tet2* loss influences hematopoietic differentiation within the myeloid progenitor compartment of *Jak2V617F* mice but is insufficient to induce leukemic transformation. (A-C) White blood cell (WBC) count, hematocrit, and platelet (PLT) count of age-matched WT, *Tet2^{null}*, *Jak2^{VF}*, and *Jak2^{VF}/*Tet2^{null}** mice 24 to 30 weeks old (mean ± SEM; n = 4 in each group). (D-F) Relative frequency of common myeloid progenitor (CMP), granulocyte macrophage progenitor (GMP), and megakaryocyte erythroid progenitor (MEP) cells in bone marrow from age-matched WT, *Tet2^{null}*, *Jak2^{VF}*, and *Jak2^{VF}/*Tet2^{null}** mice (mean ± SEM; n = 4 in each group). (G-I) Histopathologic sections of bone marrow from representative WT, *Tet2^{null}*, *Jak2^{VF}*, and *Jak2^{VF}/*Tet2^{null}** mice (original magnifications ×10 for G1-G4, ×40 for H1-H4, and ×100 for I1-I4; H&E stain).

advantage for *Jak2^{VF}/*Tet2^{null}** and *Tet2^{null}* cells (Figure 3E-F). Chimerism in the LSK compartment at 18 weeks showed that >90% of the cells were derived from *Jak2^{VF}/*Tet2^{null}** or *Tet2^{null}* donors in these groups (Figure 3G). We next determined the cell cycle status of LSK cells from primary mice from each of the genotypes. Consistent with our previously published findings,³³ we found a more activated cell cycle in *Jak2^{VF}* LSK cells compared to WT LSK cells

(supplemental Figure 5G). We also found a more activated cell cycle in both *Jak2^{VF}/*Tet2^{null}** LSK and lineage *c-Kit^{lo}/c-Kit^{hi}* cells compared to WT LSK and lineage *c-Kit^{lo}/c-Kit^{hi}* cells (supplemental Figure 5H). We have previously demonstrated that MPN disease-propagating cells are contained exclusively in the LT-HSC (CD150⁺ CD48⁻ LSK) compartment of *Jak2V617F* mice and that *Jak2V617F* expression in ST-HSCs and MPP cells does not confer

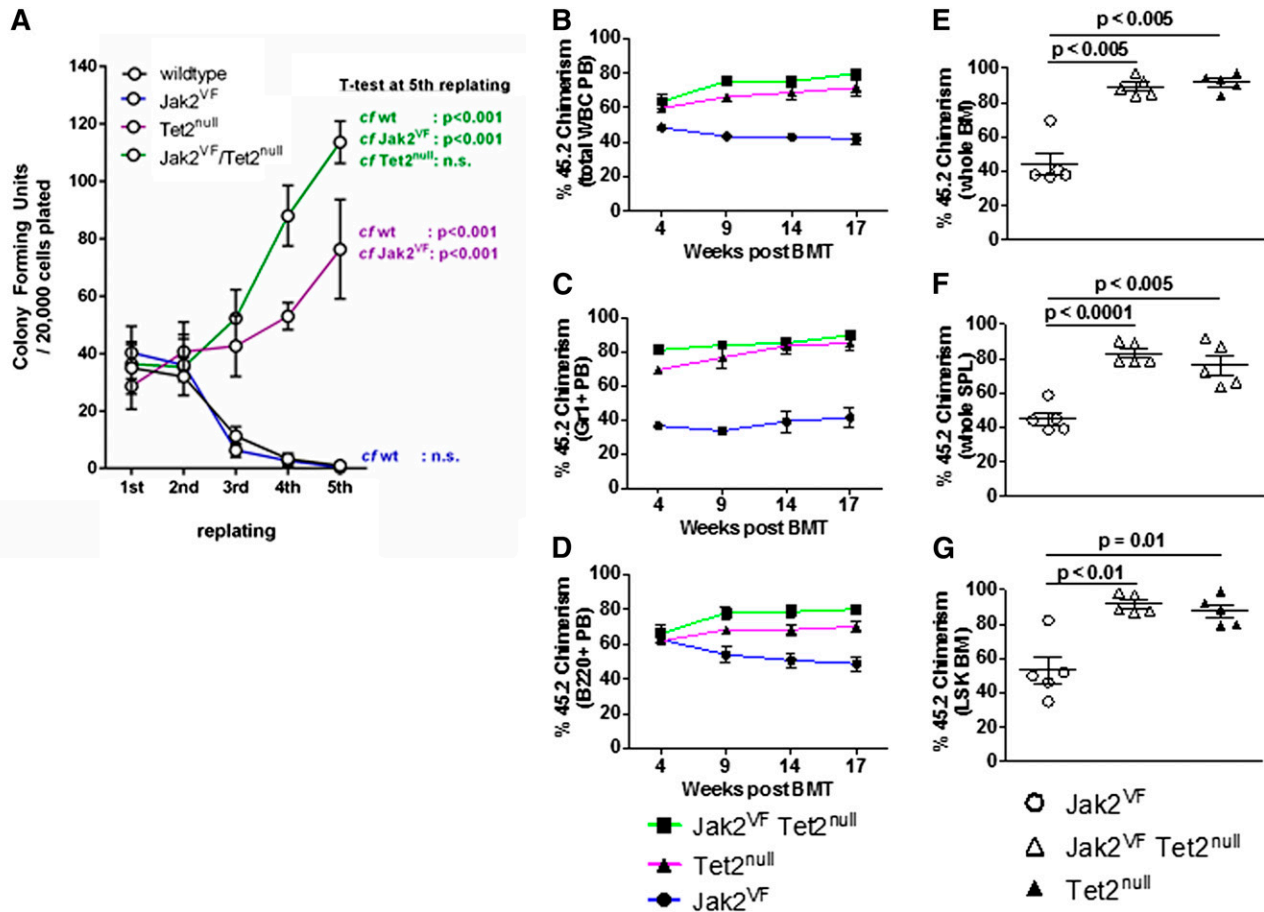


Figure 3. *Tet2* loss confers enhanced self-renewal to *Jak2V617F* HSPCs in vitro and in vivo. (A) Colony-forming unit assays from unfractionated bone marrow derived from WT, *Jak2^{VF}*, *Tet2^{null}*, and *Jak2^{VF}/Tet2^{null}* mice. Results represent the average of triplicate assays (mean \pm SEM). The percentage of 45.2 donor chimerism assessed in peripheral blood (PB) total WBCs (B), PB Gr1⁺ cells (C), and PB B220⁺ cells (D) from lethally irradiated secondary recipients of *Jak2^{VF}*, *Tet2^{null}*, or *Jak2^{VF}/Tet2^{null}* LSK cells competed against an approximately equal number of 45.1 WT LSK cells, measured 4 to 17 weeks posttransplantation (mean \pm SEM; $n = 5$ in each group). The percentage of 45.2 donor chimerism assessed in whole bone marrow (BM) cells (E), whole spleen (SPL) (F), and LSK BM cells (G) from lethally irradiated secondary recipients of *Jak2^{VF}*, *Tet2^{null}*, or *Jak2^{VF}/Tet2^{null}* LSK cells competed against an approximately equal number of 45.1 WT LSK cells, measured 18 weeks posttransplantation (mean \pm SEM; $n = 5$ in each group). *P* values for each of the comparisons are indicated in the figure.

long-term self-renewal capability to these cell populations.³⁴ To determine whether *Tet2* loss enhanced the self-renewal of *Jak2V617F*-mutant ST-HSCs or MPP cells, we compared the competitive repopulation of ST-HSCs (CD150⁺ CD48⁺ LSK) or MPP cells (CD48⁺ LSK) purified from *Jak2^{VF}* or *Jak2^{VF}/Tet2^{null}* mice using bone marrow transplantation and found no difference in self-renewal capacity between the groups at 19 weeks (supplemental Figure 3E-F). In aggregate, these data demonstrate that (1) homozygous *Tet2* loss confers a competitive advantage to *Jak2V617F*-mutant LT-HSCs similar to that seen in *Tet2*-deficient LT-HSCs that are WT for *Jak2* and (2) deleting *Tet2* in *Jak2V617F*-mutant ST-HSCs or MPP cells does not confer long-term self-renewal capability to these cell populations.

***Jak2V617F* expression and *Tet2* loss cause distinct and nonoverlapping gene expression changes**

To interrogate the molecular pathways responsible for the different HSC phenotypes of *Jak2^{VF}* and *Jak2^{VF}/Tet2^{null}* mice, we performed gene expression profiling of LSK cells derived from WT, *Jak2^{VF}*, *Tet2^{null}*, or *Jak2^{VF}/Tet2^{null}* animals ($n = 2-4$ mice per group). Unsupervised hierarchical clustering of the global gene expression signatures revealed two main branches in the gene expression hierarchy, with WT and *Tet2^{null}* samples clustering closely along one branch, and

Jak2^{VF} and *Jak2^{VF}/Tet2^{null}* samples composing the other (Figure 4A). This finding indicates that *Jak2V617F* expression imparts a larger effect on global gene expression patterns than *Tet2* loss. We successfully identified 17 unique transcripts that were differentially regulated by *Jak2V617F* expression, *Tet2* loss, or both (false discovery rate <10%; minimum fold change relative to WT samples = 1.3) (Figure 4B; supplemental Table 1). These transcripts included those unique to LSK cells harboring the *Jak2^{VF}* allele ($n = 2$), *Tet2^{null}* allele ($n = 2$), or the *Jak2^{VF}/Tet2^{null}* alleles ($n = 8$), as well as transcripts that were common to *Jak2^{VF}* and *Jak2^{VF}/Tet2^{null}* LSK cells ($n = 5$) (Figure 4B-C).

The paucity of differentially expressed genes in multiple comparisons and the modest magnitudes of the fold change suggested that individually, these genes were unlikely to be the sole drivers of the phenotypic differences in the *Jak2^{VF}*, *Tet2^{null}*, or *Jak2^{VF}/Tet2^{null}* animals. Therefore, we used GSEA to identify more subtle perturbations downstream of *Jak2V617F* expression or *Tet2* loss in LSK cells by leveraging the data set in its entirety for the presence of specific gene signatures (supplemental Tables 2 and 3). We found that targets of STAT5A signaling²⁷ were enriched among genes that were differentially expressed in *Jak2^{VF}* and *Jak2^{VF}/Tet2^{null}* LSK cells, but not in genes differentially expressed in *Tet2^{null}* LSK cells (Figure 4D). In addition, we found enrichment of genes that harbor putative STAT5 binding sites (defined by the

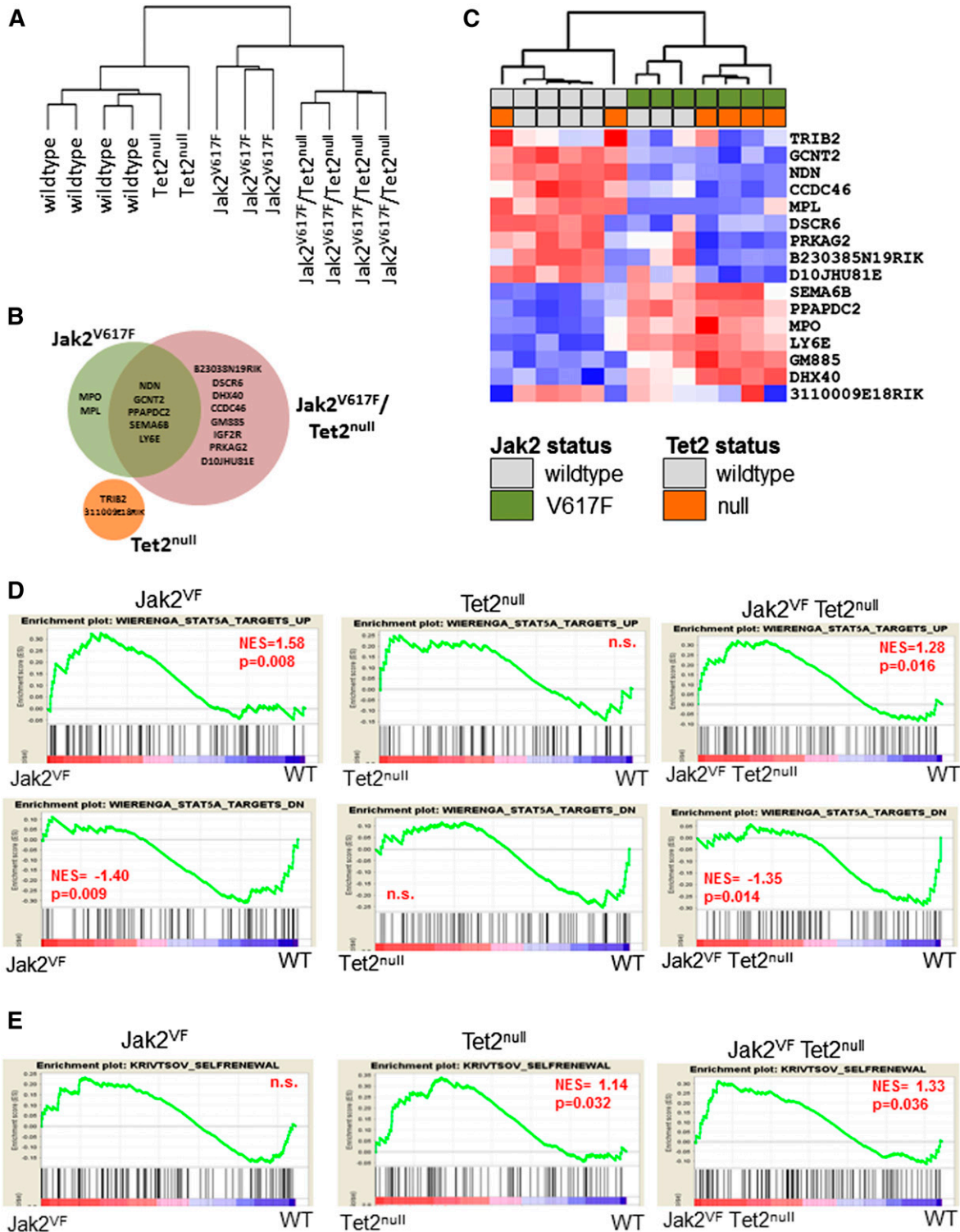


Figure 4. *Jak2*V617F expression and *Tet2* loss cause distinct and nonoverlapping gene expression changes. (A) Dendrogram constructed from unsupervised hierarchical clustering of all 13 data sets from WT (n = 4), *Tet2*^{null} (n = 2), *Jak2*^{VF} (n = 3), and *Jak2*^{VF}/*Tet2*^{null} (n = 4) LSK cells using Pearson correlation. (B) Venn diagram depicting differentially expressed genes in LSK cells from *Jak2*^{VF}, *Tet2*^{null}, and *Jak2*^{VF}/*Tet2*^{null} mice (false discovery rate = 10%; minimum fold change relative to WT samples = 1.3). (C) Hierarchical clustering of expression profiles of all 12 data sets according to the 17 genes differentially expressed in either *Jak2*^{VF}, *Tet2*^{null}, or *Jak2*^{VF}/*Tet2*^{null} mice relative to WT controls. A red/blue color scale depicts gene expression levels (red: high; blue: low). Dendrograms were constructed using Pearson correlation. (D) GSEA demonstrating enrichment for STAT5A target genes in *Jak2*^{VF} and *Jak2*^{VF}/*Tet2*^{null} LSK cells but not in *Tet2*^{null} LSK cells (top row: STAT5A targets UP; bottom row: STAT5A targets DOWN). (E) GSEA demonstrating enrichment of an HSC self-renewal signature in *Tet2*^{null} and *Jak2*^{VF}/*Tet2*^{null} LSK cells but not in *Jak2*^{VF} LSK cells. P values for each of the comparisons are indicated in the figure. NES, net enrichment score; n.s., not significant.

motif NAWTTCYN within \pm 2kb of transcriptional start site) only in mice harboring a mutant *Jak2* allele but not in *Tet2*-deleted LSK cells (supplemental Figure 6A). Concomitantly, increased STAT5A signatures were correlated with enrichment of gene signatures from erythroid-, megakaryocytic-, and granulocyte macrophage-committed precursors,³⁵ a feature of *Jak2*^{VF} and *Jak2*^{VF}/*Tet2*^{null} (but not *Tet2*^{null}) LSK cells (supplemental Figure 6B). Taken together, these findings demonstrate that the LSK compartment of mice harboring mutant *Jak2* exhibits genetic signatures indicative of robust activation of the *Jak2*-Stat5 signaling axis.

Next, we performed GSEA using a 363-gene signature that has previously been shown to be associated with a murine leukemic stem cell self-renewal signature.²⁸ We found significant enrichment of an HSC self-renewal signature in LSK cells from *Jak2*^{VF}/*Tet2*^{null} and *Tet2*^{null} mice but not in LSK cells from *Jak2*^{VF} animals (Figure 4E). These findings are consistent with our in vitro and in vivo data demonstrating both increased serial replating capacity and enhanced competitive repopulation activity for *Tet2*-deficient LSK cells, irrespective of *Jak2* status.

Discussion

MPNs are primarily disorders of activated intracellular signaling, with the majority of patients harboring mutations in genes that encode proteins that regulate cytokine signaling.⁴ The recent identification of *CALR* mutations provides further evidence that MPNs are diseases driven by aberrant signal transduction.^{3,13} Mutations in genes involved in epigenetic regulation (eg, *TET2*, *ASXL1*, *DNMT3A*, and *EZH2*) are the most frequently comutated genes with signaling mutations in MPNs,^{18,36} suggesting that genetic cooperation may occur between these two classes of genes in MPNs. *TET2* mutations are known to occur within the HSC compartment of MPN patients,³⁷ and although an initial clonal analysis of patient samples demonstrated that *TET2* mutations can precede or follow the *JAK2V617F* mutation,³⁸ a more recent larger study has shown that *TET2* mutations are predominantly acquired prior to *JAK2V617F*.¹⁸ Initial functional studies in immunodeficient mice demonstrated that *TET2*-*JAK2V617F* comutated CD34⁺ HSCs have increased repopulating capacity over *JAK2V617F*-mutated CD34⁺ HSCs.³⁷ In this study, using syngeneic genetic murine models that we have developed, we determined the individual and combinatorial effects of *Jak2V617F* expression and *Tet2* loss on (1) disease phenotype; (2) HSPC function; and (3) HSC signaling and self-renewal transcriptional signatures.

We found that homozygous *Tet2* loss accelerated the MPN phenotype of *Jak2V617F* mice, as evidenced by expansion of the splenic HSC compartment, by enhanced extramedullary hematopoiesis, and by splenomegaly. Although mutations in epigenetic regulators are enriched in more advanced phases of MPN such as myelofibrosis and secondary AML,^{14,16,18,29-31} in our study, combining a mutant *Jak2* allele with a *Tet2*^{null} allele was insufficient to induce fibrotic or leukemic transformation at 6 months of age. The fact that AML which arises out of *JAK2V617F*-mutant MPNs retains the *JAK2V617F* allele only approximately 50% of the time^{39,40} suggests that only a subset of genetic lesions seen in secondary AML cooperate with *JAK2V617F* and that cell nonautonomous mechanisms of transformation may also occur. One additional note is that in our study we used VavCre to target Cre recombinase to the hematopoietic lineage,²⁴ and in so doing, *Jak2V617F* expression and *Tet2* loss occurred simultaneously in VavCre-positive cells. In MPN patients, *JAK2V617F* and *TET2* mutations typically occur

sequentially,¹⁸ and it is possible that the order in which these mutations are acquired influences the disease phenotype. Because VavCre is noninducible, we were unable to address the impact of the temporal order of mutation acquisition on MPN phenotype.

In functional studies, we found a strong competitive advantage for *Jak2*^{VF}/*Tet2*^{null} compound mutant HSPCs, together with marked expansion of *Jak2*^{VF}/*Tet2*^{null} myeloid and erythroid precursor cell populations, resulting in an enhanced MPN phenotype in *Jak2*^{VF}/*Tet2*^{null} mice compared with *Jak2*^{VF} or *Tet2*^{null} animals. These findings are consistent with a model in which *Tet2* loss drives clonal dominance in HSCs, and *Jak2V617F* expression causes expansion of downstream progenitor and precursor cell populations, resulting in disease progression through combinatorial effects. Furthermore, these findings are consistent with the facts that the *JAK2V617F* allele burden in the HSC compartment of polycythemia vera and essential thrombocythemia patients is low and that *JAK2V617F*-mutant HSCs predominate in more advanced phases of MPNs such as myelofibrosis in which epigenetic mutations are enriched.⁴¹

The results of the functional studies outlined above are supported by our findings from the gene expression profiling of LSK cells. In this study, we found that both *Jak2V617F* expression and *Tet2* loss were associated with distinct and nonoverlapping gene expression signatures in the HSC compartment. Using GSEA, we found that a STAT5A signature was enriched only in *Jak2*^{VF} LSK cells, that an HSC self-renewal signature was enriched only in *Tet2*^{null} LSK cells, but that both signatures were enriched in *Jak2*^{VF}/*Tet2*^{null} LSK cells. These data demonstrate that *Jak2V617F* expression and *Tet2* loss each exert a specific effect on the transcriptional program of LSK cells. Specifically, *Jak2V617F* facilitates increased STAT5 signaling, which is known to potentiate erythroid differentiation, whereas *Tet2* loss gives rise to a leukemic stem cell transcriptional program that is associated with increased HSC self-renewal. The combined effects of these transcriptional changes in the HSC compartment drive the development of a more florid MPN phenotype (*Jak2*^{VF}/*Tet2*^{null} mice) compared to the phenotype that arises when either transcriptional program manifests alone (*Jak2*^{VF} or *Tet2*^{null} mice).

In conclusion, we report the effects of homozygous *Tet2* loss on *Jak2V617F*-mediated MPNs. Overall, we find accelerated myeloproliferation but no overt fibrotic or leukemic transformation. In aggregate, this work elucidates the functional effects of combined *Jak2V617F* expression and *Tet2* loss in distinct hematopoietic compartments in vivo and provides insight into the mechanisms of clonal dominance and disease progression in MPNs.

Acknowledgments

This work was supported by grants from the National Institutes of Health, National Heart, Lung, and Blood Institute (K08 HL109734) (A.M.), the MPN Foundation (A.M.), and the Leukemia Research Foundation (A.M.). A.M. has received support from the Jeanne D. Housman Fund for Research on Myeloproliferative Disorders and is a recipient of a Damon Runyon clinical investigator award. E.C. is a recipient of a Lady Tata Memorial Trust Award, and E.A.R. is a recipient of an American Society of Hematology HONORS Award.

Authorship

Contribution: A.M., E.C., R.L., and B.L.E. designed experiments and interpreted data; A.M., L.J.B., E.A.R., L.P., S.E., A.K., and K.B.

performed experiments; E.C. performed experiments and analyzed gene expression data; R.K.S. performed experiments and reviewed, interpreted, and photographed histopathology; and A.M. and E.C. wrote the manuscript. All authors reviewed the manuscript.

Conflict-of-interest disclosure: The authors declare no competing financial interests.

Correspondence: Ann Mullally, Brigham and Women's Hospital, Karp Building 5.215, 1 Blackfan Circle, Boston, MA 02115; e-mail: amullally@partners.org.

References

- Walter MJ, Shen D, Ding L, et al. Clonal architecture of secondary acute myeloid leukemia. *N Engl J Med*. 2012;366(12):1090-1098.
- Cancer Genome Atlas Research Network. Genomic and epigenomic landscapes of adult de novo acute myeloid leukemia. *N Engl J Med*. 2013;368(22):2059-2074.
- Nangalia J, Massie CE, Baxter EJ, et al. Somatic CALR mutations in myeloproliferative neoplasms with nonmutated JAK2. *N Engl J Med*. 2013;369(25):2391-2405.
- Vainchenker W, Delhommeau F, Constantinescu SN, Bernard OA. New mutations and pathogenesis of myeloproliferative neoplasms. *Blood*. 2011;118(7):1723-1735.
- Baxter EJ, Scott LM, Campbell PJ, et al; Cancer Genome Project. Acquired mutation of the tyrosine kinase JAK2 in human myeloproliferative disorders. *Lancet*. 2005;365(9464):1054-1061.
- James C, Ugo V, Le Couédic JP, et al. A unique clonal JAK2 mutation leading to constitutive signalling causes polycythemia vera. *Nature*. 2005;434(7037):1144-1148.
- Kralovics R, Passamonti F, Buser AS, et al. A gain-of-function mutation of JAK2 in myeloproliferative disorders. *N Engl J Med*. 2005;352(17):1779-1790.
- Levine RL, Wadleigh M, Cools J, et al. Activating mutation in the tyrosine kinase JAK2 in polycythemia vera, essential thrombocythemia, and myeloid metaplasia with myelofibrosis. *Cancer Cell*. 2005;7(4):387-397.
- Scott LM, Tong W, Levine RL, et al. JAK2 exon 12 mutations in polycythemia vera and idiopathic erythrocytosis. *N Engl J Med*. 2007;356(5):459-468.
- Pikman Y, Lee BH, Mercher T, et al. MPLW515L is a novel somatic activating mutation in myelofibrosis with myeloid metaplasia. *PLoS Med*. 2006;3(7):e270.
- Oh ST, Simonds EF, Jones C, et al. Novel mutations in the inhibitory adaptor protein LNK drive JAK-STAT signaling in patients with myeloproliferative neoplasms. *Blood*. 2010;116(6):988-992.
- Grand FH, Hidalgo-Curtis CE, Ernst T, et al. Frequent CBL mutations associated with 11q acquired uniparental disomy in myeloproliferative neoplasms. *Blood*. 2009;113(24):6182-6192.
- Klampfl T, Gisslinger H, Harutyunyan AS, et al. Somatic mutations of calreticulin in myeloproliferative neoplasms. *N Engl J Med*. 2013;369(25):2379-2390.
- Shih AH, Abdel-Wahab O, Patel JP, Levine RL. The role of mutations in epigenetic regulators in myeloid malignancies. *Nat Rev Cancer*. 2012;12(9):599-612.
- Abdel-Wahab O, Mullally A, Hedvat C, et al. Genetic characterization of TET1, TET2, and TET3 alterations in myeloid malignancies. *Blood*. 2009;114(1):144-147.
- Tefferi A, Pardanani A, Lim KH, et al. TET2 mutations and their clinical correlates in polycythemia vera, essential thrombocythemia and myelofibrosis. *Leukemia*. 2009;23(5):905-911.
- Soucie E, Hanssens K, Mercher T, et al. In aggressive forms of mastocytosis, TET2 loss cooperates with c-KITD816V to transform mast cells. *Blood*. 2012;120(24):4846-4849.
- Lundberg P, Karow A, Nienhold R, et al. Clonal evolution and clinical correlates of somatic mutations in myeloproliferative neoplasms. *Blood*. 2014;123(14):2220-2228.
- Rampal R, Al-Shahrour F, Abdel-Wahab O, et al. Integrated genomic analysis illustrates the central role of JAK-STAT pathway activation in myeloproliferative neoplasm pathogenesis. *Blood*. 2014;123(22):e123-e133.
- Mullally A, Lane SW, Brumme K, Ebert BL. Myeloproliferative neoplasm animal models. *Hematol Oncol Clin North Am*. 2012;26(5):1065-1081.
- Li J, Kent DG, Chen E, Green AR. Mouse models of myeloproliferative neoplasms: JAK of all grades. *Dis Model Mech*. 2011;4(3):311-317.
- Mullally A, Lane SW, Ball B, et al. Physiological Jak2V617F expression causes a lethal myeloproliferative neoplasm with differential effects on hematopoietic stem and progenitor cells. *Cancer Cell*. 2010;17(6):584-596.
- Moran-Crusio K, Reavie L, Shih A, et al. Tet2 loss leads to increased hematopoietic stem cell self-renewal and myeloid transformation. *Cancer Cell*. 2011;20(1):11-24.
- Georgiades P, Ogilvy S, Duval H, et al. VavCre transgenic mice: a tool for mutagenesis in hematopoietic and endothelial lineages. *Genesis*. 2002;34(4):251-256.
- Gould J, Getz G, Monti S, Reich M, Mesirov JP. Comparative gene marker selection suite. *Bioinformatics*. 2006;22(15):1924-1925.
- Subramanian A, Tamayo P, Mootha VK, et al. Gene set enrichment analysis: a knowledge-based approach for interpreting genome-wide expression profiles. *Proc Natl Acad Sci USA*. 2005;102(43):15545-15550.
- Wierenga AT, Vellenga E, Schuringa JJ. Maximal STAT5-induced proliferation and self-renewal at intermediate STAT5 activity levels. *Mol Cell Biol*. 2008;28(21):6668-6680.
- Krivtsov AV, Twomey D, Feng Z, et al. Transformation from committed progenitor to leukaemia stem cell initiated by MLL-AF9. *Nature*. 2006;442(7104):818-822.
- Abdel-Wahab O, Manshouri T, Patel J, et al. Genetic analysis of transforming events that convert chronic myeloproliferative neoplasms to leukemias. *Cancer Res*. 2010;70(2):447-452.
- Beer PA, Delhommeau F, LeCouédic JP, et al. Two routes to leukemic transformation after a JAK2 mutation-positive myeloproliferative neoplasm. *Blood*. 2010;115(14):2891-2900.
- Zhang SJ, Rampal R, Manshouri T, et al. Genetic analysis of patients with leukemic transformation of myeloproliferative neoplasms shows recurrent SRSF2 mutations that are associated with adverse outcome. *Blood*. 2012;119(19):4480-4485.
- Varricchio L, Mancini A, Migliaccio AR. Pathological interactions between hematopoietic stem cells and their niche revealed by mouse models of primary myelofibrosis. *Expert Rev Hematol*. 2009;2(3):315-334.
- Mullally A, Brueedigam C, Poveromo L, et al. Depletion of Jak2V617F myeloproliferative neoplasm-propagating stem cells by interferon- α in a murine model of polycythemia vera. *Blood*. 2013;121(18):3692-3702.
- Mullally A, Poveromo L, Schneider RK, Al-Shahrour F, Lane SW, Ebert BL. Distinct roles for long-term hematopoietic stem cells and erythroid precursor cells in a murine model of Jak2V617F-mediated polycythemia vera. *Blood*. 2012;120(1):166-172.
- Pronk CJ, Rossi DJ, Månsson R, et al. Elucidation of the phenotypic, functional, and molecular topography of a myeloerythroid progenitor cell hierarchy. *Cell Stem Cell*. 2007;1(4):428-442.
- Vannucchi AM, Lasho TL, Guglielmelli P, et al. Mutations and prognosis in primary myelofibrosis. *Leukemia*. 2013;27(9):1861-1869.
- Delhommeau F, Dupont S, Della Valle V, et al. Mutation in TET2 in myeloid cancers. *N Engl J Med*. 2009;360(22):2289-2301.
- Schaub FX, Looser R, Li S, et al. Clonal analysis of TET2 and JAK2 mutations suggests that TET2 can be a late event in the progression of myeloproliferative neoplasms. *Blood*. 2010;115(10):2003-2007.
- Campbell PJ, Baxter EJ, Beer PA, et al. Mutation of JAK2 in the myeloproliferative disorders: timing, clonality studies, cytogenetic associations, and role in leukemic transformation. *Blood*. 2006;108(10):3548-3555.
- Theocharides A, Boissinot M, Girodon F, et al. Leukemic blasts in transformed JAK2-V617F-positive myeloproliferative disorders are frequently negative for the JAK2-V617F mutation. *Blood*. 2007;110(1):375-379.
- Stein BL, Williams DM, Rogers O, Isaacs MA, Spivak JL, Moliterno AR. Disease burden at the progenitor level is a feature of primary myelofibrosis: a multivariable analysis of 164 JAK2 V617F-positive myeloproliferative neoplasm patients. *Exp Hematol*. 2011;39(1):95-101.